



Fluorometric determination of quercetin by using graphitic carbon nitride nanoparticles modified with a molecularly imprinted polymer

Shengnan Xu¹ · Ligang Chen¹ · Ling Ma²

Received: 21 June 2018 / Accepted: 20 September 2018 / Published online: 3 October 2018
© Springer-Verlag GmbH Austria, part of Springer Nature 2018

Abstract

The authors describe a fluorescent probe for sensitive and selective determination of quercetin, an indicator for the freshness of drinks. The probe consists of silica ball encapsulated graphitic carbon nitride (g-C₃N₄) modified with a molecularly imprinted polymer (MIP). It was synthesized via reverse microemulsion. The resulting MIP@g-C₃N₄ nanocomposite was characterized by fluorescence spectroscopy, transmission electron microscopy, Fourier transform infrared spectroscopy, and X-ray powder diffraction. Quercetin quenches the fluorescence of the MIP@g-C₃N₄ probe. The effect was used to quantify quercetin in grape juice, tea juice, black tea, and red wine by fluorometry ($\lambda_{\text{exc}} = 350 \text{ nm}$, $\lambda_{\text{em}} = 460 \text{ nm}$). Response is linear in the 10–1000 ng mL⁻¹ quercetin concentration range. The detection limit is 2.5 ng mL⁻¹, recoveries range between 90.7 and 94.1%, and relative standard deviations are between 2.1 and 5.5%.

Keywords Soft drinks · Graphite carbon nitride · Molecular imprinting · π -Interaction · Probe · Fluorescence · Flavonoids · Reverse microemulsion

Introduction

Flavonoids are widely distributed in fruits, vegetables and some drinks [1–3]. Quercetin (Fig. S1) is a typical flavonol and can be detected in some daily food such as grape, tea, onion, nuts, berries, cauliflower and cabbage [4]. So it is significant to establish an effective approach for detecting quercetin.

A number of analytical methods are used for quantitative analysis of quercetin, for instance, high-performance liquid chromatography [5], liquid chromatography-mass

spectrometry [6], capillary electrophoresis [7], electrochemical sensor [8] and fluorescence spectroscopy [9]. The above analytical methods have acquired good experimental results, but these methods have some disadvantages. For instance, the high-performance liquid chromatography method has a large reagent consumption and long analysis time. The capillary electrophoresis and electrochemical detection sometimes have poor reproducibility. Compared with other detection methods, fluorescence spectroscopy has the advantages of high sensitivity and low analysis cost.

Quantum dots (QDs), as novel fluorescent indicators, have unique optical properties that can be widely used in biomedical and pharmaceutical analysis. At present, a number of metal semiconductor QDs are applied as fluorophores in optical sensing, such as CdS [10], Mn-doped ZnS [11] and CdTe [12]. These metal semiconductor QDs have excellent fluorescence properties. But they have toxic and low selectivity. So how to fabricate benign nanomaterials with good optical properties is an interesting challenge.

In order to solve the problem of high toxicity of traditional metal QDs, some new fluorescent nanomaterials have been discovered, such as graphite carbon nitride (g-C₃N₄), carbon dots and graphene quantum dots. The synthetic steps of carbon dots and graphene quantum dots are relatively complex and the resulting product

Electronic supplementary material The online version of this article (<https://doi.org/10.1007/s00604-018-3016-y>) contains supplementary material, which is available to authorized users.

✉ Ligang Chen
ligangchen2008@163.com

✉ Ling Ma
maling63@163.com

¹ Department of Chemistry, College of Science, Northeast Forestry University, 26 Hexing Road, Harbin 150040, People's Republic of China

² College of Forestry, Northeast Forestry University, 26 Hexing Road, Harbin 150040, People's Republic of China

contains impurities. Comparatively speaking, $g\text{-C}_3\text{N}_4$ is a promising alternative to other QDs due to their advantages of strong fluorescence, uncomplex preparation process, low toxicity and excellent biocompatibility. $G\text{-C}_3\text{N}_4$, a kind of visible-light-response material similar to graphite, is a two-dimensional planar conjugation structure with unique electronic band [13]. Each layer of $g\text{-C}_3\text{N}_4$ consists of a repeating tri-s-triazine ring packaged together by van der Waals interactions [14, 15]. It has become of interest due to their unique optical properties.

In order to increase the selectivity of QDs, molecular imprinting technique was used. For example, Ren et al. used QDs coated with molecularly imprinted polymer (MIP) as fluorescence probe for detecting cyphenothrin [16]. Zhang et al. have synthesized MIP- $g/r\text{-QDs}$ as a ratiometric fluorescent probe to detect melamine [17]. Their methods have achieved good results. It is a promising analytical method that QDs combined with molecularly imprinted technology. The method has attracted more and more attention.

In this work, an eco-friendly fluorescent probe was constructed which based on $g\text{-C}_3\text{N}_4$ combined with molecular imprinting for detecting quercetin. The $g\text{-C}_3\text{N}_4$ as a fluorescent signal is environmentally friendly and uncomplicated in preparation. The fluorescence probe can detect quercetin based on photoinduced electron transfer fluorescence quenching mechanism. Under the optimal conditions, the probe for quercetin assay was validated, and then was successfully applied to drink samples analysis.

Experimental

Materials and reagents

The standard reagent of melamine was purchased from Aladdin (Shanghai, China, <http://www.aladdin-e.com>). Dihydrate sodium citrate, citric acid monohydrate, 3-aminopropyltriethoxysilane, kaempferol, galangin, myricetin and bisphenol A were bought from Aladdin (Shanghai, China, <http://www.aladdin-e.com>). TEOS, n-amyl alcohol, ethanol, triton X-100, methanol, ammonium hydroxide, sodium hydroxide were purchased from Kermel (Tianjin, China, <http://www.chemreagent.com/>). Cyclohexane was purchased from Guangfu (Tianjin, China, <http://tjguangfu.company.lookchem.cn>). High-purity water was purchased from a Milli-Q water system (Millipore, Billerica, MA, USA, <http://www.merckmilliporechina.com>). Beverages and red wines were bought from Harbin supermarket. All reagents were analytical grade.

Preparation of the graphitic carbon nitride nanoparticles modified with a molecularly imprinted polymer (MIP@ $g\text{-C}_3\text{N}_4$)

The $g\text{-C}_3\text{N}_4$ was synthesized according to the available methods in the literature [18]. The MIP@ $g\text{-C}_3\text{N}_4$ composite was synthesized at room temperature via reverse microemulsion. First, 20 mL of cyclohexane, 3.6 mL of Triton X-100, 4.4 mL of n-amyl alcohol and 1.0 mL of distilled water were stirred for 5 min. The $g\text{-C}_3\text{N}_4$ (0.1 g) was added the above solution, then stirring 30 min in room temperature. Second, 200 μL of TEOS and 100 μL of $\text{NH}_3\cdot\text{H}_2\text{O}$ were added to above reaction solution. The mixture was stirred for 10 h so that the $g\text{-C}_3\text{N}_4$ was successfully encapsulated with silicon. Third, 0.1 g of quercetin (disperse in 20 mL of ethanol) and 250 μL of APTES were added to the system for stirring 1 h. Afterwards, 500 μL of TEOS and 1 mL of $\text{NH}_3\cdot\text{H}_2\text{O}$ were added in the microemulsion and stirred for 12 h under avoiding light. The MIP@ $g\text{-C}_3\text{N}_4$ composite was synthesized, and washed with ethanol and water. Finally, methanol/acetic acid (9:1, v/v) was used to elute template molecule.

The same procedure was used to simultaneously prepare the non-imprinted appended to $g\text{-C}_3\text{N}_4$ (NIP@ $g\text{-C}_3\text{N}_4$) without addition of the template quercetin.

Characterization

The Fourier transform infrared spectrum (FT-IR) was received by using FT-IR360 spectrometer (Nicolet, Madison, WI, USA, <http://www.chem17.com>). The X-ray diffraction (XRD) spectrum was received by using a Shimadzu XRD-600 diffractometer (Kyoto, Japan, <https://www.shimadzu.com>). Topography was received by using the H7650 transmission electron microscope (TEM) (Hitachi, Japan, <http://www.hitachi.com>). The ultraviolet spectrum (UV) was received by using TU-1901 spectrometer (PERSEE, Beijing, China, <http://www.instrument.com>). At the room temperature, fluorescence spectrum was received by using F-4600 fluorescence spectrophotometer (Hitachi, Japan, <https://www.antpedia.com>). X-ray Photoelectron Spectroscopy (XPS) spectrum (The United States, Minnesota, <http://www.phl.com/index.html>) was received by using PHI 5700 ESCA System, that the pass energy of wide scan and narrow scan were 187.85 eV and 23.50 eV, respectively. The MIP@ $g\text{-C}_3\text{N}_4$ were dissolved in citric acid-sodium citrate buffer by A KQ5200E ultrasonic instrument (Kunshan Instrument, Kunshan, China, <http://www.ks-csyq.com>).

Fluorometry

By using a 400 nm excitation filter, a fluorescence spectrum was achieved in the wavelength range of 400–

700 nm with an excitation wavelength of 350 nm. All measurements were performed under the following parameters: the slit width was 10 nm; the scan speed was 240 nm min^{-1} ; and photomultiplier tube voltage was 550 V. Moreover, every sample was repeated measurement three times under the same conditions, the Quartz cell of 1 cm path length was used for fluorescence measurement. The different concentrations of quercetin solutions were mixed with 0.1 mg mL^{-1} MIP@g-C₃N₄ solution (1:1, v/v) that adjusted to pH = 3 by citrate buffer (0.1 mol L^{-1}). After the reaction was completed, the fluorescence analysis was carried out.

Analysis of quercetin in real samples

The quercetin content in the beverage and red wine are one of the signs of the quality of related products. Some kinds of juices and red wines from local supermarkets were analyzed for investigating the applicability of the MIP@g-C₃N₄ method. The red wine samples were diluted 10 times before further treatment due to the high content of quercetin. The samples were treated by the following process: MIP@g-C₃N₄ (0.1 mg mL^{-1}) was dispersed in citric acid-sodium citrate buffer at pH = 3. The samples (10 mL) was mixed with the 0.1 mg mL^{-1} MIP@g-C₃N₄ (10 mL). After full shocking for 5 min, centrifuging and discarding the supernatant, the mixture was washed with distilled water (3 mL) to remove impurities for example sugar. Finally, the MIP@g-C₃N₄ adsorbing quercetin was redispersed in citrate buffer (20 mL) for fluorescence measurement. The fluorescence emission spectra were recorded under a 350 nm excitation wavelength and the fluorescence intensity of the maximum emission peak at 460 nm was used for the quantitative analysis of quercetin. Then the concentrations of quercetin in drink samples will be gained according to the linear equation.

Results and discussion

Choice of materials

Numerous nanomaterials are used as fluorescent probes for trace detection, such as metal QDs, g-C₃N₄, carbon dots and graphene QDs. The synthesis step of carbon dots is complicated and accompanied by a large amount of impurities [19]. The use of natural graphite or metal catalysts for the synthesis of graphene QDs can result in residual metal impurities (e.g., Fe, Co, and Ni) that are not easily removed [20]. Metal QDs are toxic and not environmentally friendly. In comparison, the synthesis step of g-C₃N₄ is uncomplex, and the product has high purity [18]. The surface of the g-C₃N₄ has many amino functional groups, which can further interact with the

analyte. Therefore, g-C₃N₄ was selected as fluorescent component. In this experiment, molecular imprinting technique was also introduced to increase the selectivity of g-C₃N₄ (Fig. 1).

The emission wavelength of g-C₃N₄ was 460 nm. Quercetin had a weak peak at an emission wavelength of 530 nm. When quercetin and g-C₃N₄ were mixed, there was no interference to the experiment.

Characterizations of g-C₃N₄ and MIP@g-C₃N₄

As estimated from the TEM images in Fig. 2a, b, the diameter of g-C₃N₄ is approximately 10 nm. In this study, the bulk g-C₃N₄ turns into small nanoparticles by ultrasound for 10 h. The role of ultrasound is to destroy van der Waals forces among the layers of g-C₃N₄. Similar experimental phenomena also have been verified in the previous literature [21]. The diameter of MIP@g-C₃N₄ is 200–500 nm, and MIP@g-C₃N₄ have regular spherical shapes.

The characterization XRD patterns of g-C₃N₄ and MIP@g-C₃N₄ are presented in Fig. 2c, d. Figure 2c is consistent with the previous reports on g-C₃N₄ [22]. The strong shoulder peak around 27.4° represent the characteristic interplanar stacking peak of conjugated aromatic systems, index for the (002) peak of g-C₃N₄. Another the weak diffraction peak around 13.07° derives from an in-planar structural packing motif, index the (100) peak of g-C₃N₄. MIP@g-C₃N₄ appears widely peaks in Fig. 2d, it may be caused by wrapping the blotting membrane.

The chemical structures and composition of g-C₃N₄ and MIP@g-C₃N₄ are further investigated by XPS measurement. The obvious peaks of C, N and O can be seen in Fig. 2e. The binding energy peaks at 286.5, 402.1 and 534.9 eV correspond to C1s, N1 s and O1s, respectively. The XPS of the composites are shown in Fig. 2f, there are five obvious peaks can be clearly observed, their peaks appear on 287.3 (C1s), 535.6 (O1s), 401.8 (N1 s), 104.8 (Si2p), 157.2 (Si2s).

FT-IR (Fig. 2g, h) spectroscopy is acquired via a Fourier transform infrared spectrometer with the KBr pellet technique. The typical functional group of g-C₃N₄ is shown in Fig. 2g. Distinct bands can be observed between 1200 and 1680 cm^{-1} and near 815 cm^{-1} , it is the result of the organic molecules containing three azine ring structures. The absorption bands appear on 1570 and 1630 cm^{-1} are attributed to C=N stretching, the bands present to 1250 , 1320 and 1410 cm^{-1} are consistent with aromatic C-N stretching, the terminal amino groups broad band appear in the 3000 – 3500 cm^{-1} , for instance, -NH₂ or =NH groups of g-C₃N₄. The sharp band of the bending vibration of characteristics of triazine rings appears in 815 cm^{-1} . The FT-IR spectroscopy of MIP@g-C₃N₄ in Fig. 2h, the characteristic peak at 3270 cm^{-1} is corresponding to the stretching vibration of the N-H and O-H bonds. A wide peak located at 1060 cm^{-1} is corresponding to Si-O stretching

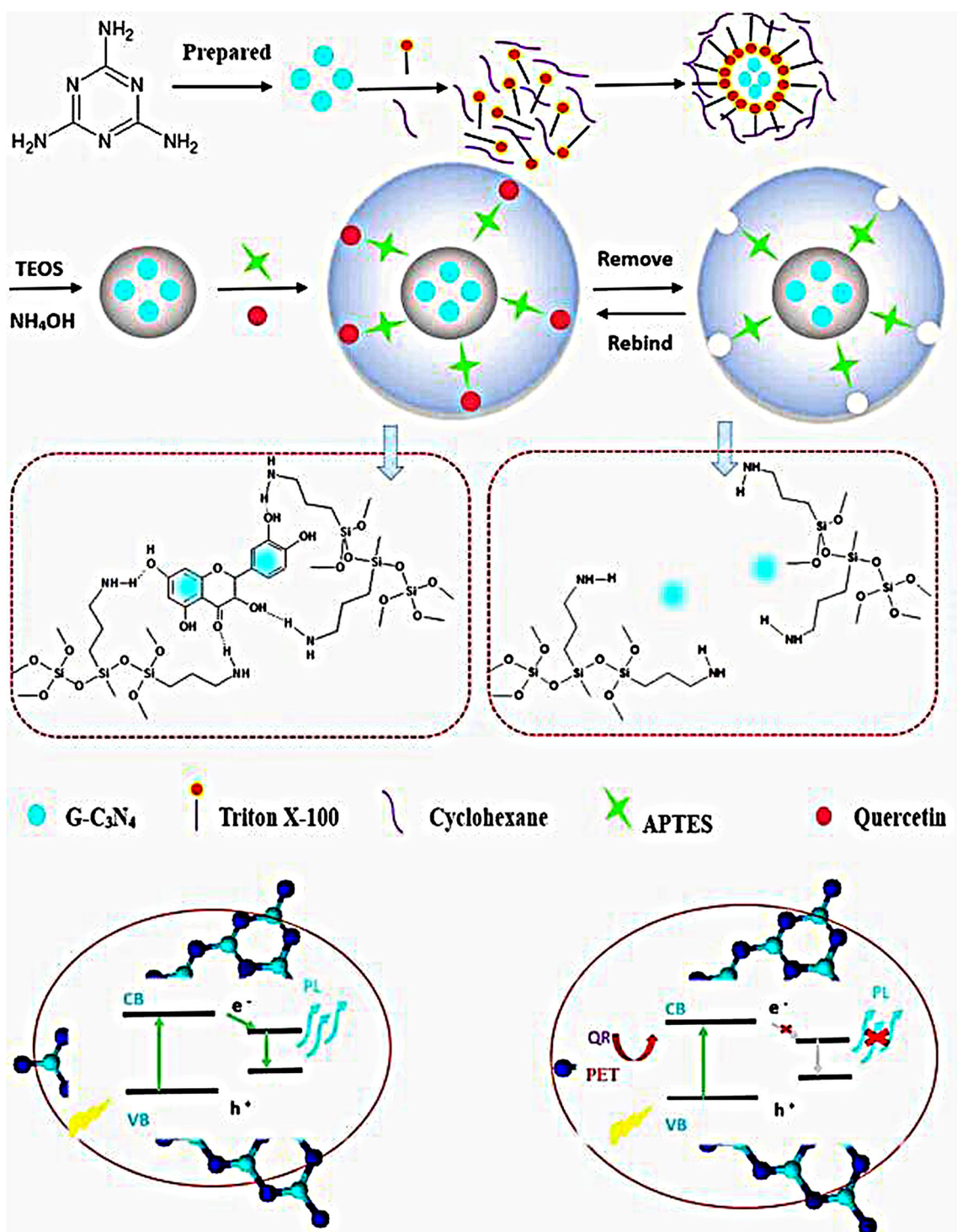


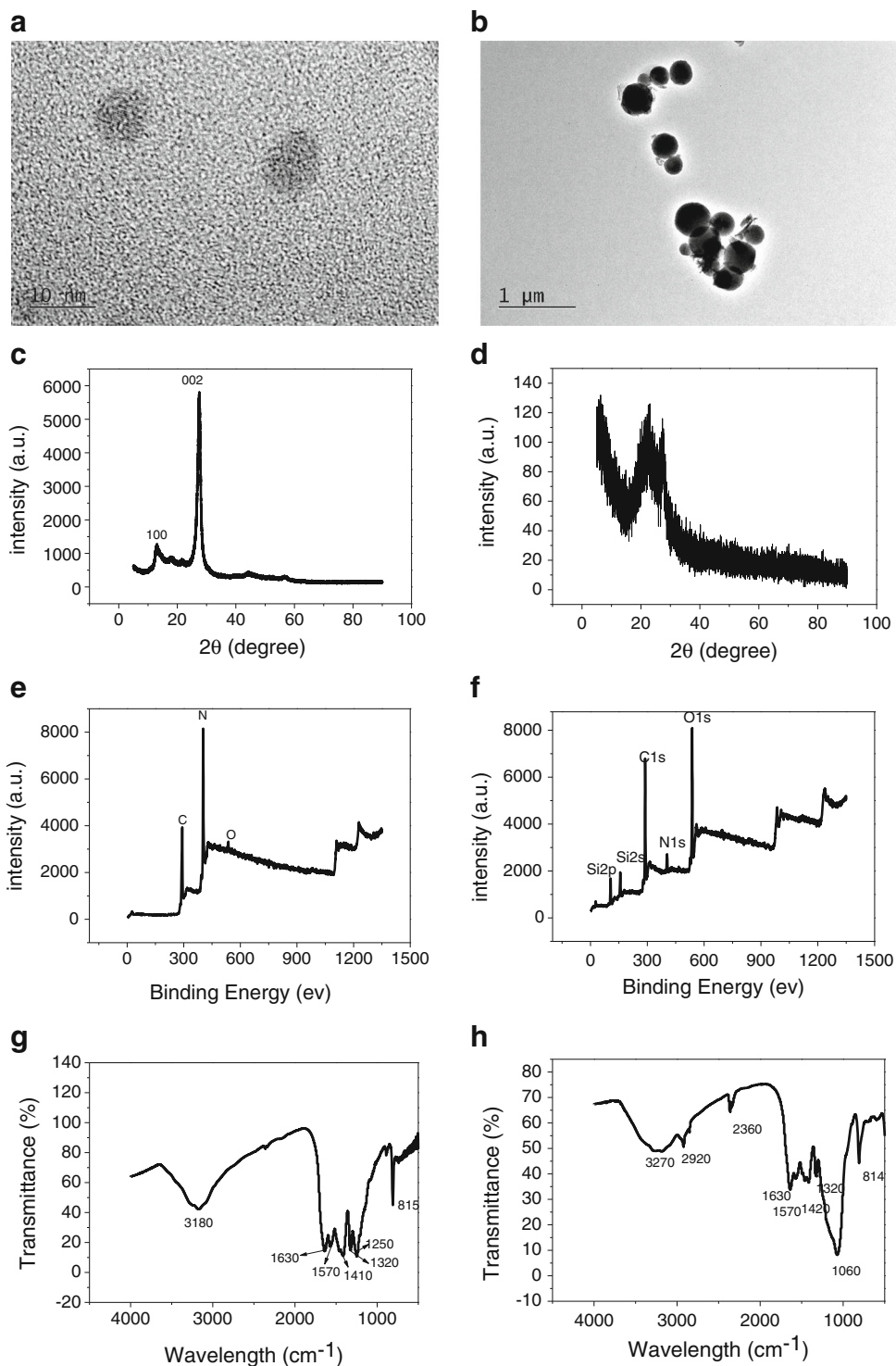
Fig. 1 Schematic of the synthesis of graphitic carbon nitride nanoparticles modified with a molecularly imprinted polymer (MIP@g-C₃N₄) including the preparation and modification of g-C₃N₄ and further encapsulation of molecularly imprinted polymers on g-C₃N₄

vibration. The C=N stretching vibrations are observed at 1630 and 1570 cm⁻¹, respectively. The stretching vibration of Si-H (2360 cm⁻¹) and -CH₃ of APTES (2920 cm⁻¹), indicated MIP is successfully combined with g-C₃N₄.

Optimization of method

The following parameters were optimized: (a) Sample pH value; (b) Reaction time (c) Concentration of

Fig. 2 Transmission electron microscopy images of g-C₃N₄ (a) and MIP@g-C₃N₄ (b). X-ray powder diffraction of g-C₃N₄ (c) and MIP@g-C₃N₄ (d), X-ray Photoelectron Spectroscopy of g-C₃N₄ (e) and MIP@g-C₃N₄ (f), Fourier transform infrared spectroscopy of g-C₃N₄ (g) and MIP@g-C₃N₄ (h)



MIP@g-C₃N₄. Respective data and Figures are given in the Electronic Supporting Material in Fig. S2, Fig. S3 and Fig. S4. In short, the following experimental conditions were found to give best results: (a) Best sample pH value: pH=3; (b) Optimal reaction time: 5 min; (c) Optimal concentration of MIP@g-C₃N₄: 0.1 mg mL⁻¹.

The response of MIP@g-C₃N₄ and NIP@g-C₃N₄ to quercetin

The effects of different concentrations of quercetin on imprinted and nonimprinted probes (MIP@g-C₃N₄ and NIP@g-C₃N₄) is shown in Figure 3. It indicates that the

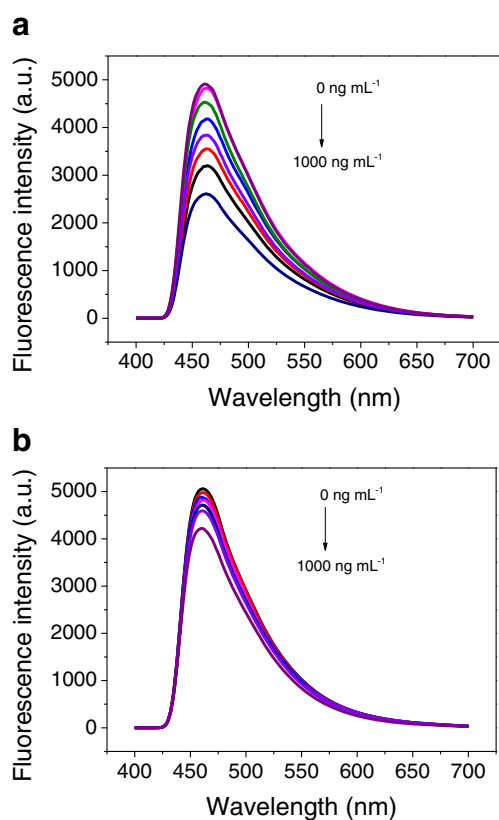


Fig. 3 Fluorescence spectra of MIP@g-C₃N₄ (a) and NIP@g-C₃N₄ (b) with different concentrations of quercetin ($\lambda_{exc} = 350$ nm, pH = 3, reaction time: 5 min)

fluorescence of MIP@g-C₃N₄ and NIP@g-C₃N₄ decreased as the concentration of quercetin increased. The specific interactions between quercetin and MIP@g-C₃N₄ are the main reason of fluorescence quenching. It is obvious that the decline of the fluorescent intensity of the MIP@g-C₃N₄ is larger than that of NIP@g-C₃N₄ after adding the same concentration of quercetin. The different fluorescence quenching intensity can be explained by the Stern–Volmer [23]:

$$F_0/F = 1 + K_{sv}[Q] \quad (1)$$

In the equation, F_0 is the initial fluorescence of MIP@g-C₃N₄ without quercetin, F is the fluorescence of MIP@g-C₃N₄ after adding quercetin, K_{sv} is the Stern–Volmer constant, and $[Q]$ is the different quercetin concentrations added. Quercetin with a concentration range of 2–2000 ng mL⁻¹ was tested. In the experiment, when the concentration of quercetin is less than 10 ng mL⁻¹, the fluorescence quenching is too small and the repeatability is poor. When the concentration of quercetin is higher than 1000 ng mL⁻¹, the linear plot greatly deviates. Quercetin shows a good linear relationship in a range of 10–1000 ng mL⁻¹. As shown in Fig.

S5, fluorescence changes of MIP@g-C₃N₄ after adding different quercetin concentrations can be confirmed a good linear correlation between F_0/F and quercetin concentration in the range of $F_0/F = 0.000882[Q] + 1.00229$, the correlation coefficient (R^2) was 0.9994, the limit of detection (LOD) is the ratio of 3σ to K , where σ is the standard deviation of blank measurements ($n = 11$) and K is the slope of the calibration plot. The LOD of this method is 2.5 ng mL⁻¹. The imprinting factor (IF) is also calculated, through defined by the ratio of $K_{sv, MIP}$ to $K_{sv, NIP}$ (IF = 5.04). The above results are shown wide linear range and low detection limit of the prepared fluorescence probe based on MIP@g-C₃N₄.

Selective responding on MIP@g-C₃N₄

To test the selectivity of the MIP@g-C₃N₄ prepared by our method, some substances were measured, for instance, kaempferol, galangin, myricetin as the similar structures analogue, and bisphenol A as the reference compound that also contained two benzene ring and hydroxy. Their chemical structures are shown in Fig. S6. The results of Fig. S7 indicate that the MIP@g-C₃N₄ displays the highest specific recognition ability for quercetin compare with other four substances. On account of the structures of four substances are different with quercetin, when the template molecule is removed, cavity sites that match quercetin are left, these analogues can't retain in the recognition cavities of MIP@g-C₃N₄. So, quercetin can be specifically recognized by MIP@g-C₃N₄. The effect of interfering substances in the solution is investigated, and the results shows that within a certain concentration range is immune to interference (Table. S1).

Reuse is an important factor for fluorescent MIP. Fig. S8 shows the MIP@g-C₃N₄ can be used at least five times.

Fluorescence quenching mechanism

Fluorescence is reduced by various molecular interactions, excited-state reactions, molecular rearrangements, energy transfer, formation of ground state complexes, and collisional quenching, which is called fluorescence quenching. The mechanism of action of MIP@g-C₃N₄ and quercetin can be listed as follows:

- (1) There are some ways to cause fluorescence quenching such as fluorescence resonance energy transfer (FRET), photoinduced electron transfer (PET) and inner filter effect (IFE). Generally, in the FRET or IFE process, there should be a good spectral overlap between the absorption

Table 1 Thermodynamic parameters of the MIP@g-C₃N₄ with the quercetin system

T(K)	K _{sv} (L mol ⁻¹)	ΔG° (kJ mol ⁻¹)	ΔH° (kJ mol ⁻¹)	ΔS° (J mol ⁻¹ K ⁻¹)
298	2.67 × 10 ⁵	-30.95	-15.45	52
308	2.17 × 10 ⁵	-31.47		
318	1.97 × 10 ⁵	-32.23		

spectrum of quercetin and the emission spectrum of MIP@g-C₃N₄. It can be seen from Fig. S9, the peaks of the two substances do not overlap, which proves that their quenching mechanism are not FRET or IFE.

- (2) Fluorescence quenching usually has static quenching and dynamic quenching, which can be distinguished by measuring the relationship between quenching constant and temperature. The static quenching is caused by the formation of a non-luminescent ground state complex between the fluorescent molecule and the quencher. Therefore, when the temperature increases, the complex becomes unstable, resulting in the decreased of the quenching constant. The dynamic quenching is caused by collisions between quenchers and fluorophores. When the temperature rises, the collision is aggravated, leading to the quenching constant increases. As displays in Fig. S10, as the temperature increases, the quenching constant decreases. This imply that the reaction mechanism was static quenching [24].
- (3) Fluorescence quenching can also be discussed from molecular interactions (for electrostatic force, π-π, and hydrogen bonding interactions). The quercetin is added into the MIP@g-C₃N₄ solution, the molecular interactions between quercetin and MIP@g-C₃N₄ are occurred, such as electrostatic force and π-interactions, the interaction of quercetin and MIP@g-C₃N₄ is researched by using the Stern-Volmer equation in different temperatures. The thermodynamic equation as follows [25]:

$$\Delta G^O = -RT \ln K_{sv} \quad (2)$$

$$\Delta G^O = \Delta H - T \Delta S \quad (3)$$

By rearranging Eqs. 2 and 3, K_{SV} can also be calculated:

$$\ln K_{sv} = \frac{\Delta S^O}{R} - \frac{\Delta H^O}{RT} \quad (4)$$

Among them, ΔG° is free enthalpy change, ΔH° is enthalpy change, and ΔS° is entropy change. The thermodynamic equations can be used to calculate these values. The known quantities in the equation are temperature (quenching temperature in kelvin), the universal gas constant (R = 8.314 J mol⁻¹ K⁻¹), and equilibrium constant at the corresponding temperature. In Table 1, we can see the values of ΔH° = -15.45 kJ mol⁻¹ and ΔS° = 52 J mol⁻¹ K⁻¹. These data show that the interaction between the two substances is electrostatic force [24]. When a large amount of cross-linking monomer is used in the presence of the template, special recognition pores are formed due to form hydrogen bonds between the amino group of APTES and the hydroxyl group of quercetin. Quercetin can be specifically identified by special pores.

Analytical application

To validate the practical utility of the fluorescent probe, three beverages samples and four red wines samples were selected for quantitative determination of quercetin. It can be seen that quercetin is detected in the green grape juice, black tea and four red wine samples in Table 2. The concentration of quercetin in the green grape juice is

Table 2 Determination results of quercetin in drink samples (n = 3)

Drinks	Detected (ng mL ⁻¹)	Added (ng mL ⁻¹)	Found (ng mL ⁻¹)	Average recovery (%)	RSD ^a (%)
Green grape	18.0	10.0	27.7	91.0	2.3
Tea π juice	Not detected	10.0	9.8	92.2	3.1
Black tea	15.5	10.0	25.3	90.7	4.4
Red wine 1 ^b	300.5	200.0	510.0	92.4	4.3
Red wine 2 ^b	210.0	200.0	400.7	94.1	5.5
Red wine 3 ^b	273.0	200.0	467.0	92.8	2.1
Red wine 4 ^b	290.4	200.0	492.0	90.9	3.3

^a RSD is the recovery based on three calculations

^b The red wine samples were diluted 10 times

Table 3 Comparison of quercetin determination with different detection methods

Detection method	Pretreatment method	LOD (ng mL ⁻¹)	RSD (%)	Recovery (%)	Ref.
HPLC-UV	Solid-phase extraction	0.26	3.5	97.0	[26]
HPLC-UV	Ionic liquid-based cloud-point extraction	2.0	3.7	100–108	[27]
HPLC	Solid-phase extraction	510	3.6	97.2	[28]
HPLC-DAD	Solid-phase extraction	0.25		89.4–90.4	[29]
Electrochemical detection	MIP/GO/GC	14.4	0.52–2.89	97.4–101.4	[30]
Fluorescence	MIP@g-C ₃ N ₄	2.5	2.1–5.5	90.7–94.1	This work

18.0 ng mL⁻¹ and black tea is 15.5 ng mL⁻¹. four red wine samples' concentration of quercetin are 3.0, 2.1, 2.7, 2.9 μg mL⁻¹, respectively. Quercetin (10 ng mL⁻¹ and 2000 ng mL⁻¹) is added to beverages and red wines samples, respectively. The recoveries are 90.7–94.1% with relative standard deviations of 2.1–5.5%. The results indicate that MIP@g-C₃N₄ possesses good accuracy in real sample analysis.

Compared with the traditional method of detecting quercetin in Table 3, fluorescence analysis has many advantages, such as low analysis cost and short sample analysis time. Some HPLC detection methods are lower than our detection limit, but the instrument has some disadvantages of wasting reagents and requiring a long analysis time. At the same time, the specificity of detection is increased by using molecularly imprinted techniques.

The fluorescence analysis method has limitations, such as, the need for working in the UV ($\lambda_{exc} = 350$ nm) makes the probe prone to interferences by biomatter which always display strong background UV absorption and fluorescence. In addition, the UV light used for excitation may be screened off by UV absorbing biomolecules. In the future, we will find ways to solve these problems.

Conclusion

In conclusion, an effective fluorescence probe method is presented by using g-C₃N₄ combined with MIP and used to determine quercetin in beverages and red wines. The quercetin content is successfully detected in green grape juice, black tea and all kinds of red wines. Fluorescence spectroscopy has the advantages of low analysis cost and short sample analysis time. Compared with metal QDs, g-C₃N₄ has superior physicochemical and photochemical stabilities, nontoxicity, large surface area, plentiful material source and inexpensive to synthesize. In the future, we will devote to use the novel fluorescence probe to detect more food samples.

Acknowledgments This project was funded by the Fundamental Research Funds for the Central Universities (No. 2572017 EB08), Harbin science and technology innovation talent research special funds (2016RAQXJ151) and Natural Science Foundation of Heilongjiang Province (JJ2018ZR0081).

Compliance with ethical standards The author(s) declare that they have no competing interests.

References

- Nimse SB, Pal D (2015) Free radicals, natural antioxidants, and their reaction mechanisms. *RSC Adv* 5:27986–28006
- Duan Q, Cao J, Zhang J (2012) Analysis of phenolic acids and their antioxidant activity by capillary electrophoresis-mass spectrometry with field-amplified sample injection. *Anal Methods* 4:3027–3032
- Tu B, Liu ZJ, Chen ZF, Ouyang Y, Hu YJ (2015) Understanding the structure-activity relationship between quercetin and naringenin: in vitro. *RSC Adv* 5:106171–106181
- Azzi J, Jrajaj A, Auezova L, Fourmentin S, Greige-Gerges H (2018) Novel findings for quercetin encapsulation and preservation with cyclodextrins, liposomes, and drug-in-cyclodextrin-in-liposomes. *Food Hydrocoll* 81:328–340
- Berger LM, Wein S, Blank R, Metges CC, Wolfram S (2012) Bioavailability of the flavonol quercetin in cows after intraruminal application of quercetin aglycone and rutin. *J Dairy Sci* 95:5047–5055
- Zafari S, Sharifi M, Chashmi NA (2018) A comparative study of biotechnological approaches for producing valuable flavonoids in *prosopis farcta*. *Cytotechnology* 70:603–614
- Zhang HJ, Kang MQ, Zhang HQ, Yu Y (2014) Matrix solid phase dispersion extraction for determination of flavonoids in the flower of *chrysanthemum morifolium ramat* by capillary zone electrophoresis. *Anal Methods* 6:766–773
- Yao Z, Yang X, Liu X, Yang Y, Hu Y, Zhao Z (2018) Electrochemical quercetin sensor based on a nanocomposite consisting of magnetized reduced graphene oxide, silver nanoparticles and a molecularly imprinted polymer on a screen-printed electrode. *Microchim Acta* 185:70
- Zuo P, Xiao D, Gao M, Peng J, Pan R, Xia Y, He H (2014) Single-step preparation of fluorescent carbon nanoparticles, and their application as a fluorometric probe for quercetin. *Microchim Acta* 181:1309–1316
- Wang Y, Bian F, Qin XF, Wang QQ (2018) Visible light photoelectrochemical aptasensor for chloramphenicol by using a TiO₂ nanorod array sensitized with Eu (III)-doped CdS quantum dots. *Microchim Acta* 185:161
- Tan L, Chen KC, Huang C, Peng RF, Luo XY, Yang R, Cheng YF, Tang YW (2015) A fluorescent turn-on detection scheme for alpha-

- fetoprotein using quantum dots placed in a boronate-modified molecularly imprinted polymer with high affinity for glycoproteins. *Microchim Acta* 182:2615–2622
12. Song YY, Xu GH, Wei FD, Cen Y, Sohail M, Shi ML, Xu XM, Ma YS, Ma YJ, Hu Q (2018) Aptamer-based fluorescent platform for ultrasensitive adenosine detection utilizing Fe₃O₄ magnetic nanoparticles and silver nanoparticles. *Microchim Acta* 185:139
 13. Chen J, Chen Q, Chen J, Qiu H (2016) Magnetic carbon nitride nanocomposites as enhanced peroxidase mimetics for use in colorimetric bioassays, and their application to the determination of H₂O₂ and glucose. *Microchim Acta* 183:3191–3199
 14. Hu YL, Yang DL, Yang C, Feng N, Shao ZW, Zhang L, Wang XD, Weng LX, Luo ZM, Wang LH (2018) A novel "off-on" fluorescent probe based on carbon nitride nanoribbons for the detection of citrate anion and live cell imaging. *Sensors* 18:1163
 15. Zhou ZX, Shen YF, Li Y, Liu AR, Liu SQ, Zhang YJ (2015) Chemical cleavage of layered carbon nitride with enhanced photoluminescent performances and photoconduction. *ACS Nano* 9:12480–12487
 16. Ren XH, Chen LG (2015) Quantum dots coated with molecularly imprinted polymer as fluorescence probe for detection of cyphenothrin. *Biosens Bioelectron* 64:182–188
 17. Zhang L, Chen LG (2018) Visual detection of melamine by using a ratiometric fluorescent probe consisting of a red emitting CdTe core and a green emitting CdTe shell coated with a molecularly imprinted polymer. *Microchim Acta* 185:135
 18. Ho WK, Zhang ZZ, Xu MK, Zhang XW, Wang XX, Yu H (2015) Enhanced visible-light-driven photocatalytic removal of NO: effect on layer distortion on g-C₃N₄ by H₂ heating. *Appl Catal B Environ* 179:106–112
 19. Amin N, Afkhami A, Hosseinzadeh L, Madrakian T (2018) Green and cost-effective synthesis of carbon dots from date kernel and their application as a novel switchable fluorescence probe for sensitive assay of Zoledronic acid drug in human serum and cellular imaging. *Anal Chim Acta* 1030:183–193
 20. Yang SL, Li YR, Wang SF, Wang M, Chu MF, Xia BY (2018) Advances in the use of carbonaceous materials for the electrochemical determination of persistent organic pollutants. A review. *Microchim Acta* 185:112
 21. Bian W, Zhang H, Yu Q, Shi MJ, Shuang SM, Cai ZW, Choi MM (2016) Detection of Ag⁺ using graphite carbon nitride nanosheets based on fluorescence quenching. *Spectrochim Acta A* 169:122–127
 22. Zhang YW, Liu JH, Wu G, Chen W (2012) Porous graphitic carbon nitride synthesized via direct polymerization of urea for efficient sunlight-driven photocatalytic hydrogen production. *Nanoscale* 4: 5300–5303
 23. Zhang XH, Gao RQ, Li DP, Yin HY, Zhang JL, Cao HY, Zheng XF (2015) Study on interaction between 5-Bromo-4-thio-2'-deoxyuridine and human serum albumin by spectroscopy and molecular docking. *Spectrochim Acta A* 136:1775–1781
 24. Wang YQ, Zhang HM, Zhang GC, Tao WH, Tang SH (2007) Interaction of the flavonoid hesperidin with bovine serum albumin: a fluorescence quenching study. *J Lumin* 126:211–218
 25. Li XW, Li CY, Chen LG (2015) Preparation of multifunctional magnetic-fluorescent nanocomposites for analysis of tetracycline hydrochloride. *New J Chem* 39:9976–9982
 26. Ranjbari E, Biparva P, Hadjmohammadi MR (2012) Utilization of inverted dispersive liquid-liquid microextraction followed by HPLC-UV as a sensitive and efficient method for the extraction and determination of quercetin in honey and biological samples. *Talanta* 89:117–123
 27. Rasoolzadeh F, Hashemi P, Serenkeh FN (2017) Ionic liquid-based cloud-point extraction of quercetin for its sensitive HPLC-UV determination in juice samples. *Acta Chromatogr* 29:1–4
 28. Rajauria G (2018) Optimization and validation of reverse phase HPLC method for qualitative and quantitative assessment of polyphenols in seaweed. *J Pharm Biomed Anal* 148:230–237
 29. Wang LC, Shangguan YN, Hou XD, Jia Y, Liu SJ, Sun YS, Guo Y (2017) Zinc oxide crystal whiskers as a novel sorbent for solid-phase extraction of flavonoids. *J Chromatogr B* 1060:91–96
 30. Yola ML, Gupta VK, Eren T, Sen AE, Atar N (2014) A novel electro analytical nanosensor based on graphene oxide/silver nanoparticles for simultaneous determination of quercetin and morin. *Electrochim Acta* 120:204–211